

Pharmacokinetics Modeling Course

Physiologically-based pharmacokinetics models



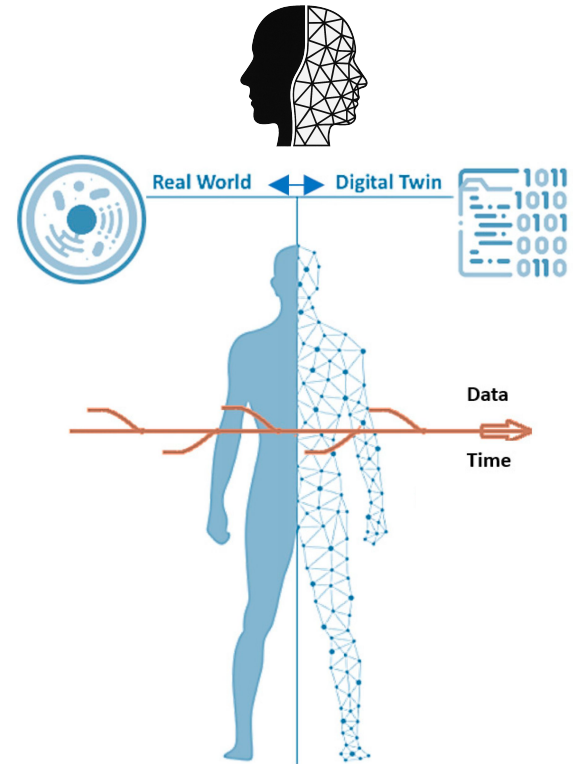
Dr. Matthias König
 Humboldt-University Berlin
 Systems Medicine of the Liver
 koenigmx@hu-berlin.de
<https://livermetabolism.com>

By the end of this section, you should be able to:

1. **Understand the structure and purpose of PBPK models** in pharmacokinetics.
2. **Differentiate** physiologically based models from **traditional compartment models**.
3. **Identify key components** of PBPK models, including **organs, tissues, blood flow**, and **drug-specific parameters** (e.g., partition coefficients, clearance).
4. **Learn how PBPK models simulate ADME processes (Absorption, Distribution, Metabolism, Excretion)** using physiological and physicochemical data.
5. **Explore key applications** of PBPK modeling in **dose prediction, special populations** (e.g., pediatric, renal/hepatic impairment), and **drug-drug interactions (DDIs)**.

Digital Twins

- A **virtual representation of a patient** that integrates **multidimensional, patient-specific information**
- **Mechanistic computational models** that enable **personalized predictions** based on **patient data**
- **Continuous updates** between the **real world** and the **digital twin**
- Used to **support medical decision-making**



Physiological based pharmacokinetic (PBPK) models

Digital Twin

● Human physiology
in silico

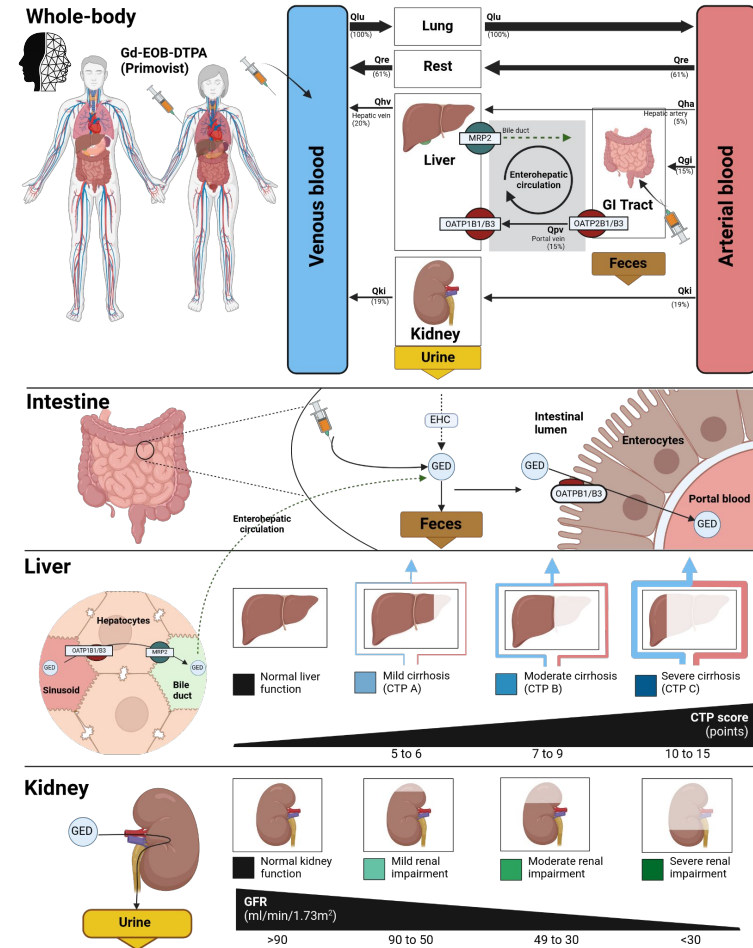
ADME

- Absorption
- Distribution
- Metabolism
- Elimination

Multi-Scale models

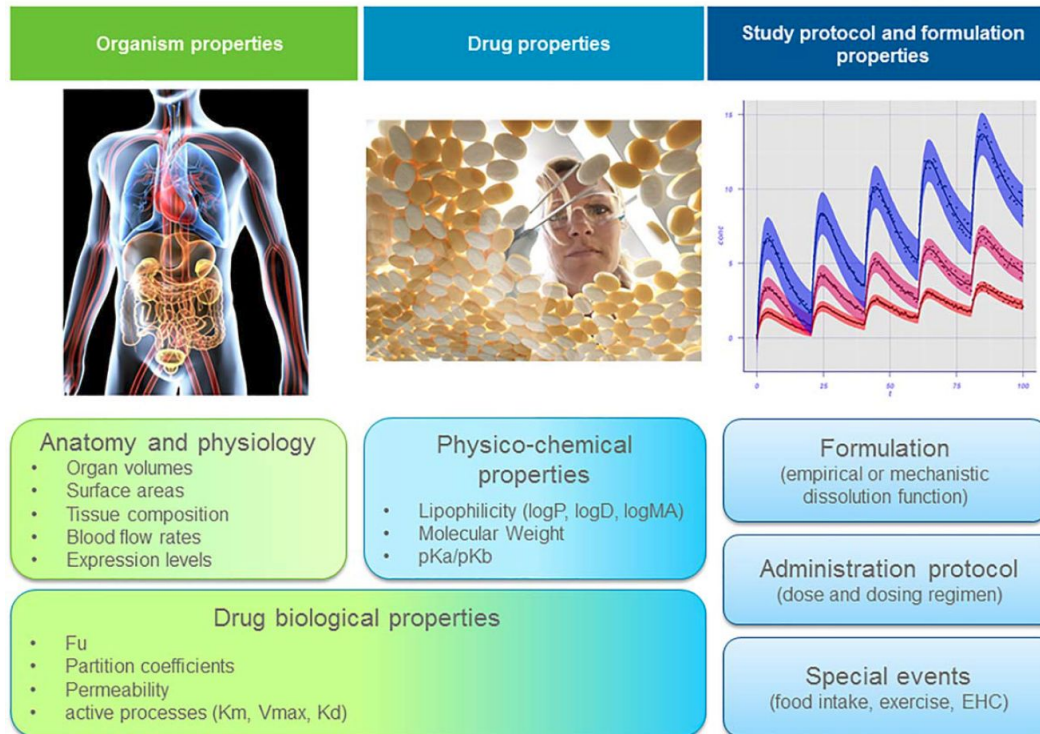
High clinical relevance

- Individualisation & Stratification
- Pathophysiology



PBPK Models

Building blocks of a PBPK model



Compartments

- organs

State variables

- drug & metabolite amounts

Ordinary Differential equations (ODE) & rules

- Blood flows, Transport, Disposition
- Metabolism, Elimination
- Absorption

Parameters

- Tissue partition coefficients
- Protein binding
- Kinetic parameter (transport & elimination)
- Blood flows, organ volumes, ...

PBPK Applications

Cross-Species Extrapolation

PBPK models can be used to facilitate the extrapolation of knowledge generated in various preclinical species to humans

In silico drug



Special Populations

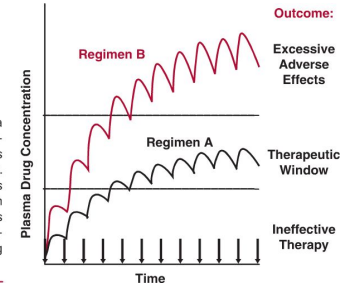
By including the appropriate physiological information, PBPK models can be used to make predictions in special populations

Drug Drug Interactions (DDI)

Thanks of the explicit inclusion of enzymatic processes, the combination of two or more models allow the prediction of interaction between drugs

Individual Dosing

FIGURE 1-4. When a drug is given in a fixed dose and at fixed time intervals (denoted by the arrows), it accumulates within the body until a plateau is reached. With regimen A, therapeutic success is achieved although not initially. With regimen B, the therapeutic objective is achieved more quickly, but the drug concentration is ultimately too high, resulting in excessive adverse effects.



Advanced Applications

PBPK models can also be integrated in more complex models such as multiscale modelling or statistical modelling, using methods such as Bayesian approaches

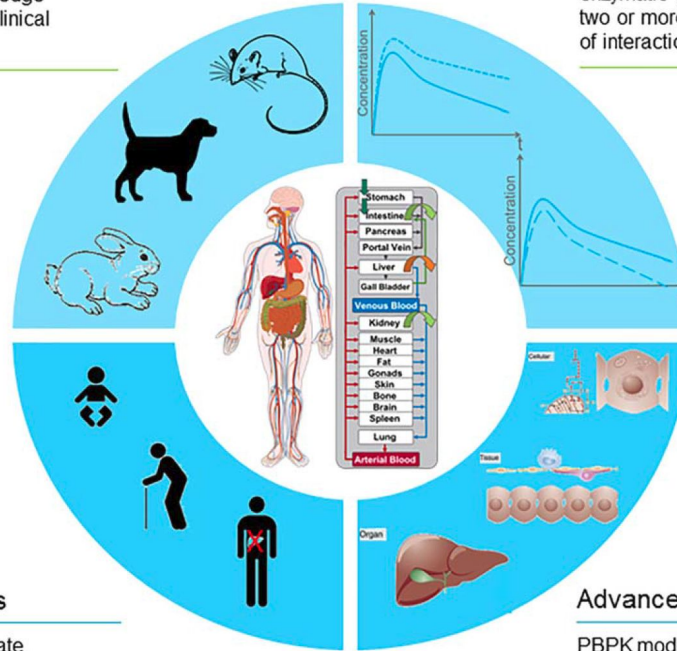
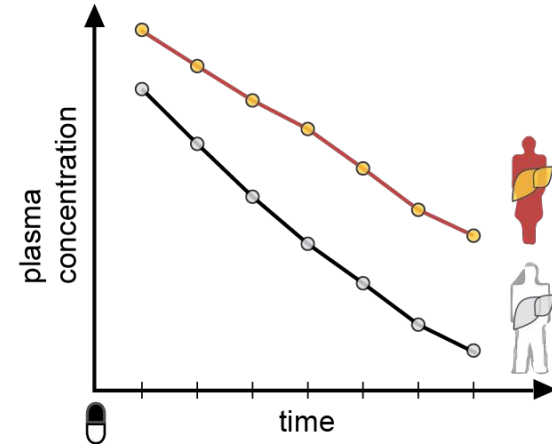
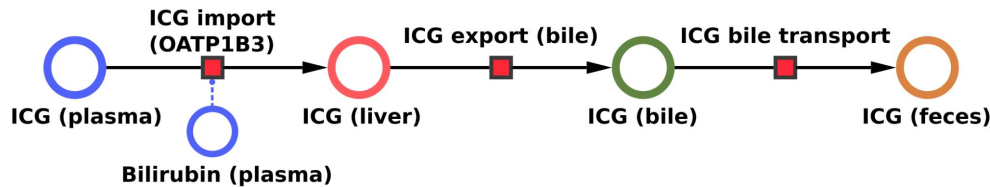
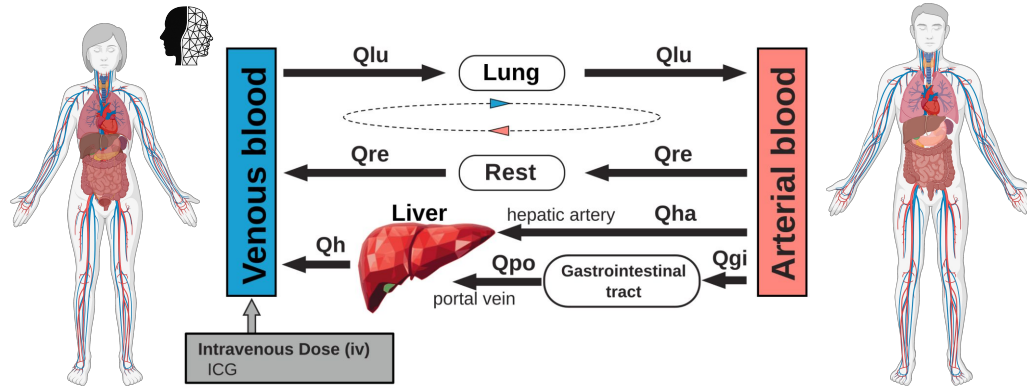


Figure 3 Schematic representation of the most common applications of PBPK modeling.

Liver function tests: Indocyanine green (ICG)



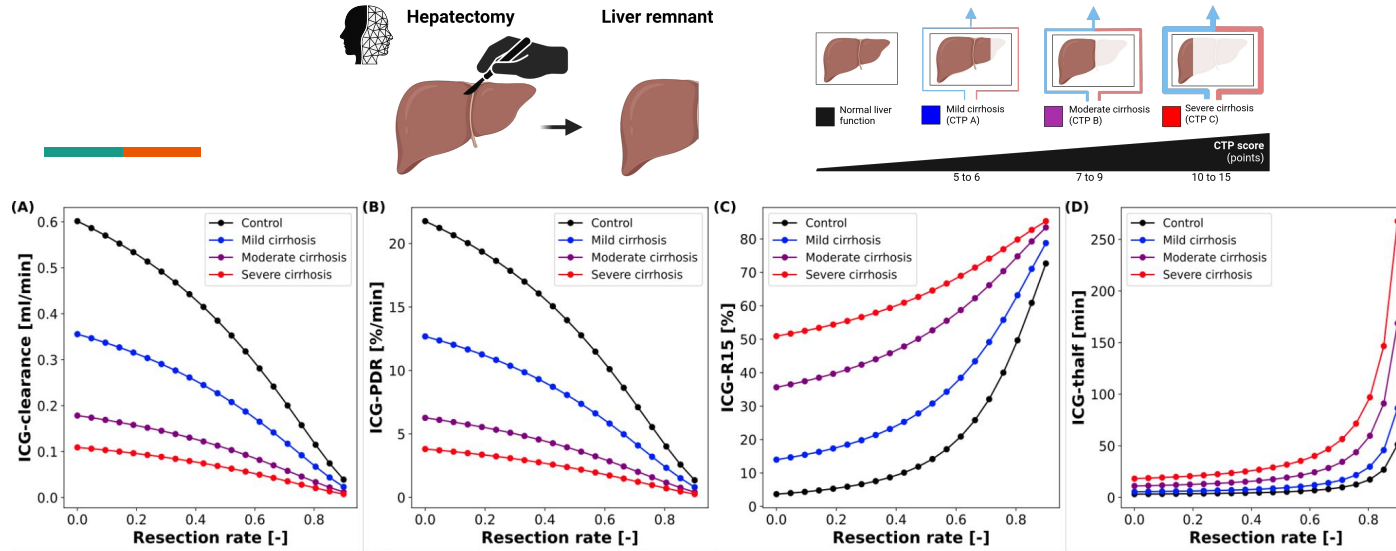
- **Anthropometric factors** (age, weight, sex)
- **Physiological factors** (Blood flow, liver volume)
- **Liver disease** (cirrhosis)
- **Surgical interventions** (hepatectomy)

Prediction of survival after hepatectomy using a physiologically based pharmacokinetic model of indocyanine green liver function tests. A Köller, J Grzegorzewski, MH Tautenhahn, **M König**. Front. Physiol., 22 November 2021; doi: [10.3389/fphys.2021.730418](https://doi.org/10.3389/fphys.2021.730418)

Physiologically based modeling of the effect of physiological and anthropometric variability on indocyanine green based liver function tests. A Köller, J Grzegorzewski, **M König**. Front Physiol. 2021 Nov 22;12:757293. doi: [10.3389/fphys.2021.757293](https://doi.org/10.3389/fphys.2021.757293). eCollection 2021.



In silico hepatectomy



A Köller, J Grzegorzewski, MH Tautenhahn, **M König**
Prediction of survival after hepatectomy using a physiologically based pharmacokinetic model of indocyanine green liver function tests.

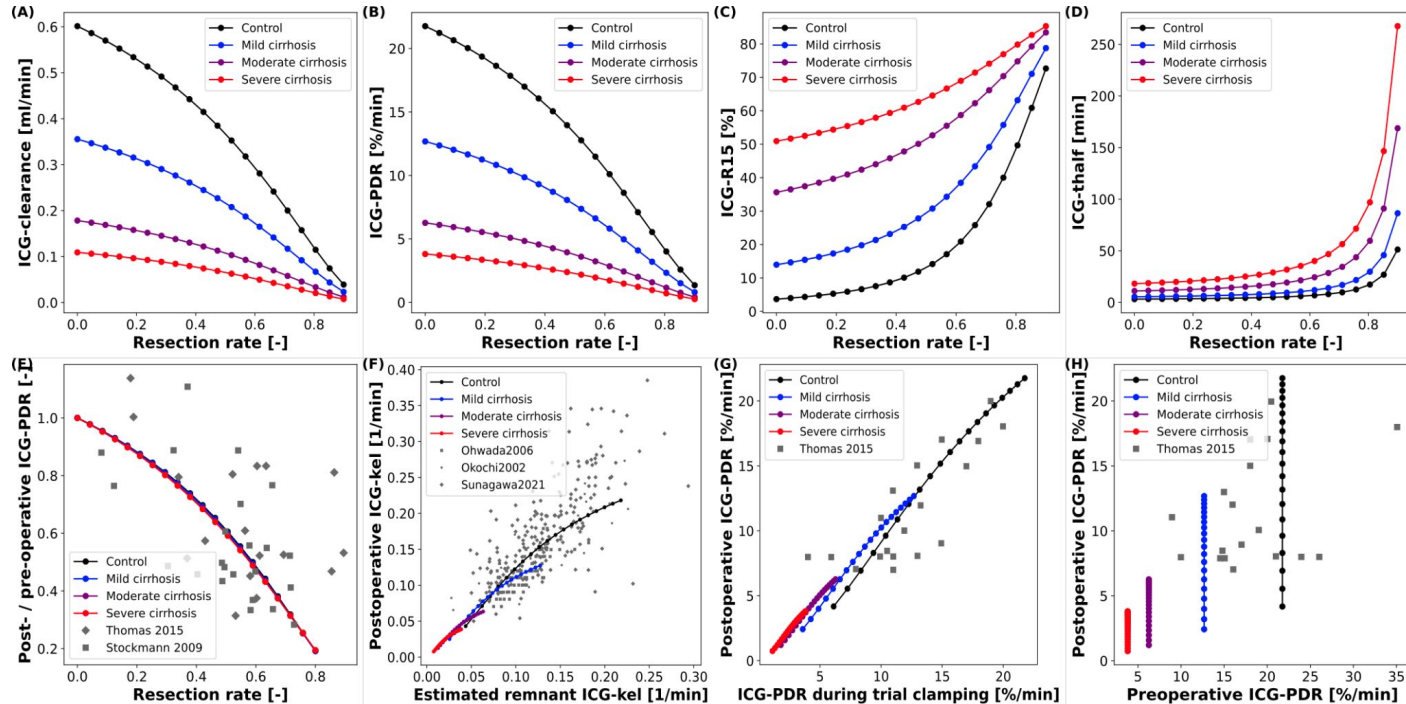
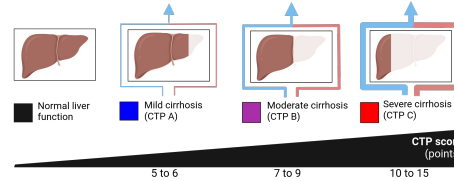
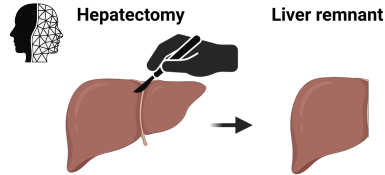
Front. Physiol., 22 November 2021; doi: [10.3389/fphys.2021.730418](https://doi.org/10.3389/fphys.2021.730418)

A Köller, J Grzegorzewski, **M König**
Physiologically based modeling of the effect of physiological and anthropometric variability on indocyanine green based liver function tests

Front Physiol. 2021 Nov 22;12:757293. doi: [10.3389/fphys.2021.757293](https://doi.org/10.3389/fphys.2021.757293). eCollection 2021.



Validation



A Köller, J Grzegorzewski, MH Tautenhahn, **M König**
Prediction of survival after hepatectomy using a physiologically based pharmacokinetic model of indocyanine green liver function tests.

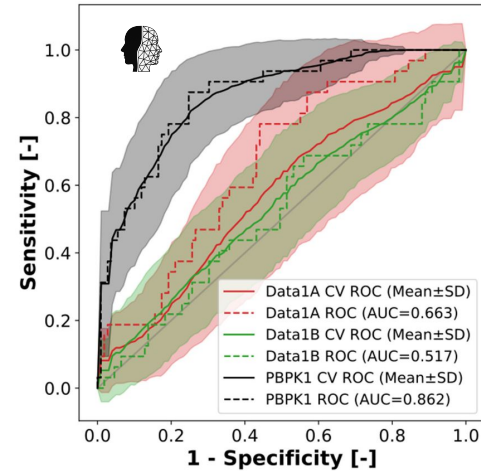
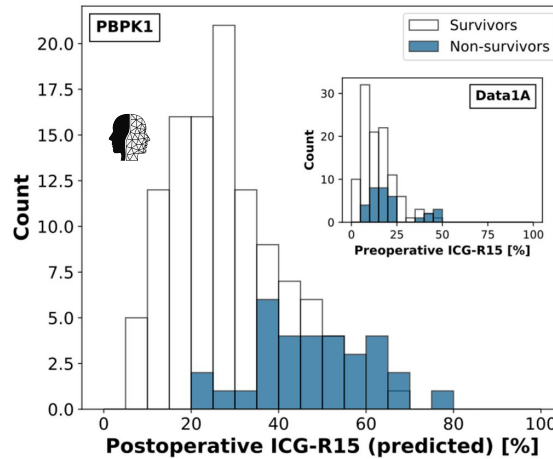
Front. Physiol., 22 November 2021; doi: [10.3389/fphys.2021.730418](https://doi.org/10.3389/fphys.2021.730418)

A Köller, J Grzegorzewski, **M König**
Physiologically based modeling of the effect of physiological and anthropometric variability on indocyanine green based liver function tests

Front Physiol. 2021 Nov 22;12:757293. doi: [10.3389/fphys.2021.757293](https://doi.org/10.3389/fphys.2021.757293). eCollection 2021.




Risk prediction after hepatectomy



Prediction with a Digital Twin (PBPK) is better than using data alone.

TABLE | Evaluation metrics for classification models of survival after hepatectomy.

Classification model	Data1A	Data1B	PBPK1 
Features	Preoperative ICG-R15	Postoperative ICG-R15 (calculated)	Postoperative ICG-R15 (predicted)
ROC AUC	0.663 (0.555 ± 0.072)	0.517 (0.481 ± 0.052)	0.862 (0.753 ± 0.090)
Balanced accuracy	0.562 (0.555 ± 0.072)	0.515 (0.481 ± 0.052)	0.761 (0.753 ± 0.090)
F1-score	0.267 (0.243 ± 0.152)	0.143 (0.118 ± 0.126)	0.611 (0.587 ± 0.136)
Precision (PPV)	0.462 (0.443 ± 0.295)	0.300 (0.192 ± 0.227)	0.550 (0.538 ± 0.152)
Recall	0.188 (0.182 ± 0.133)	0.094 (0.170 ± 0.273)	0.688 (0.681 ± 0.172)
NPV	0.797 (0.792 ± 0.067)	0.779 (0.745 ± 0.133)	0.901 (0.898 ± 0.057)

A Köller, J Grzegorzewski, MH Tautenhahn, **M König**
Prediction of survival after hepatectomy using a physiologically based pharmacokinetic model of indocyanine green liver function tests.

Front. Physiol., 22 November 2021; doi: [10.3389/fphys.2021.730418](https://doi.org/10.3389/fphys.2021.730418)

A Köller, J Grzegorzewski, **M König**
Physiologically based modeling of the effect of physiological and anthropometric variability on indocyanine green based liver function tests

Front Physiol. 2021 Nov 22;12:757293. doi: [10.3389/fphys.2021.757293](https://doi.org/10.3389/fphys.2021.757293). eCollection 2021.



Risk prediction after hepatectomy

Personalized prediction of survival after hepatectomy <https://icg-model.streamlit.app/>

Patient 

Liver disease

Liver cirrhosis

- ☐ No cirrhosis
- ☒ Mild (CPT A)
- ☐ Moderate (CPT B)
- ☐ Severe (CPT C)

Anthropometric parameters

Body weight [kg]

79

Age [yr]

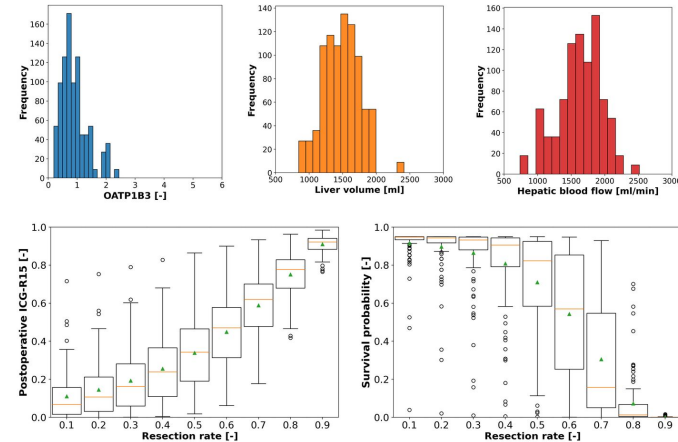
55

Liver parameters

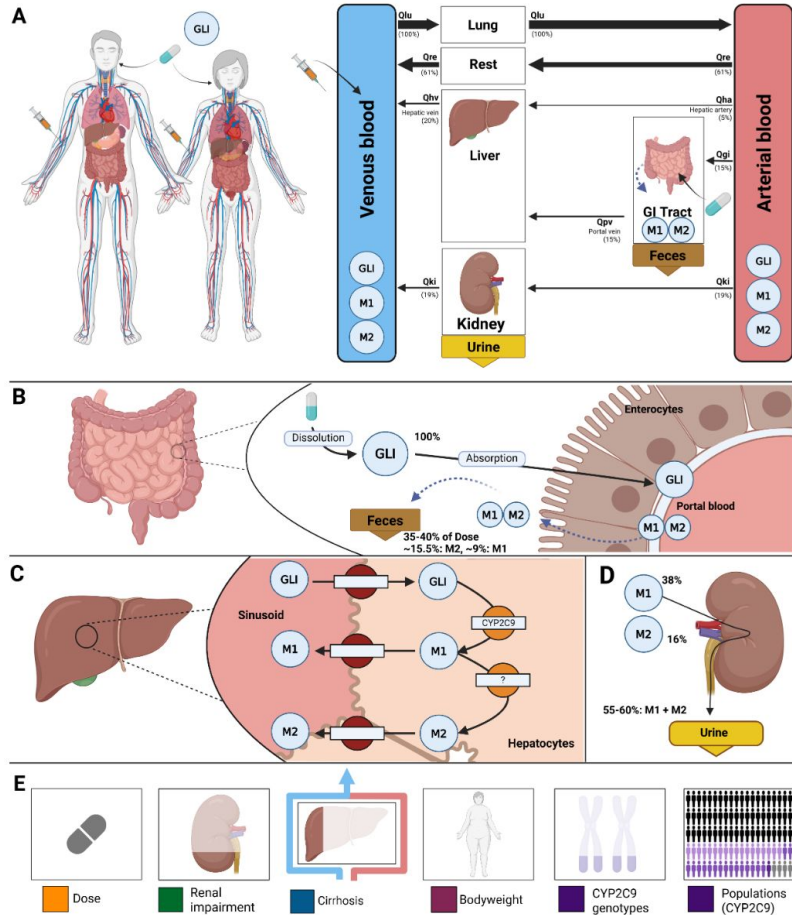
Liver volume [ml]

Hepatic blood flow [ml/min]

Personalized predictions



Glimepiride



Administration

Route: Oral (tablet).
Dosing: 1–8 mg once daily.
Tmax: 2.4–3.7 hours (rapid absorption).
Bioavailability: High, unaffected by food.

Metabolism

Pathway: Hepatic via CYP2C9.
Metabolites:

- M1: Partially active (30% of drug activity).
- M2: Inactive.

Prolonged effect: M1 extends glucose-lowering action.

Distribution

Volume of distribution: Small (8.8 L).
Plasma binding: ~99.4% to albumin.
Tissue penetration: Limited due to high binding.

Excretion

Urine: ~60% of metabolites.
Feces: ~40% of metabolites.
Parent drug: <1% in feces.
Half-life: 5–8 hours; effect lasts ~24 hours due to M1.

Fig. 1 Whole-body PBPK model of glimepiride and key factors influencing its disposition. **A)** Whole-body model illustrating glimepiride (GLI) administration (oral and intravenous), its systemic circulation via venous and arterial blood, and the key organs (liver, kidney, GI tract) involved in GLI metabolism, distribution, and excretion. **B)** Intestinal model showing dissolution and absorption of GLI by enterocytes. No enterohepatic circulation of M1 and M2 is assumed, but reverse transport via enterocytes is included. **C)** Hepatic model depicting CYP2C9-mediated metabolism of GLI to M1 and M2. **D)** Renal model highlighting the elimination of M1 and M2 via urine; unchanged GLI is not excreted renally. **E)** Key factors influencing glimepiride disposition accounted for by the model: liver function (cirrhosis), renal impairment, CYP2C9 genotypes, bodyweight, and administered dose.

Glimepiride - Dose Dependency

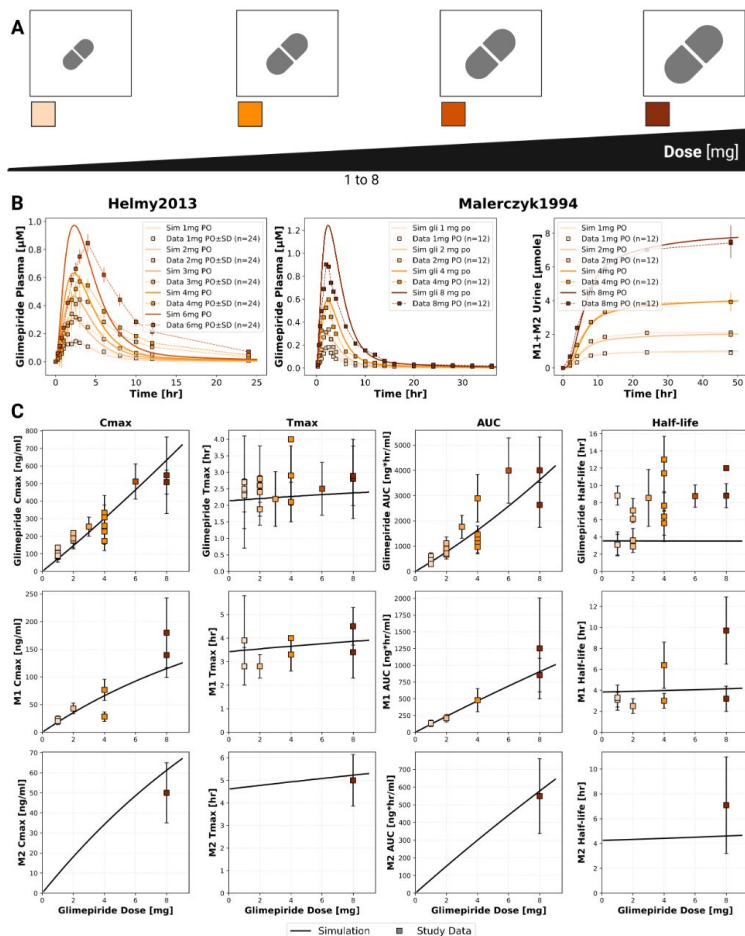


Fig. 2 Dose-dependent pharmacokinetics of glimepiride and its metabolites. A) Illustration of the glimepiride oral dose range (1-8 mg) evaluated in the simulations. **B)** Simulated (solid lines) versus observed (squares) plasma concentration-time profiles of glimepiride from Helmy et al. [19] (left), and glimepiride plasma concentrations and cumulative M1+M2 urinary excretion from Malerczyk et al. [25] (middle and right, respectively) across various oral doses (PO). Observed data are presented as mean \pm SD. **C)** Dose-dependency relationships for key pharmacokinetic parameters for glimepiride, M1, and M2. Simulation results (solid lines) are compared with experimental data (squares with error bars, representing mean \pm SD where available) aggregated from all 19 clinical studies used in the model development.

Glimepiride - Renal Impairment

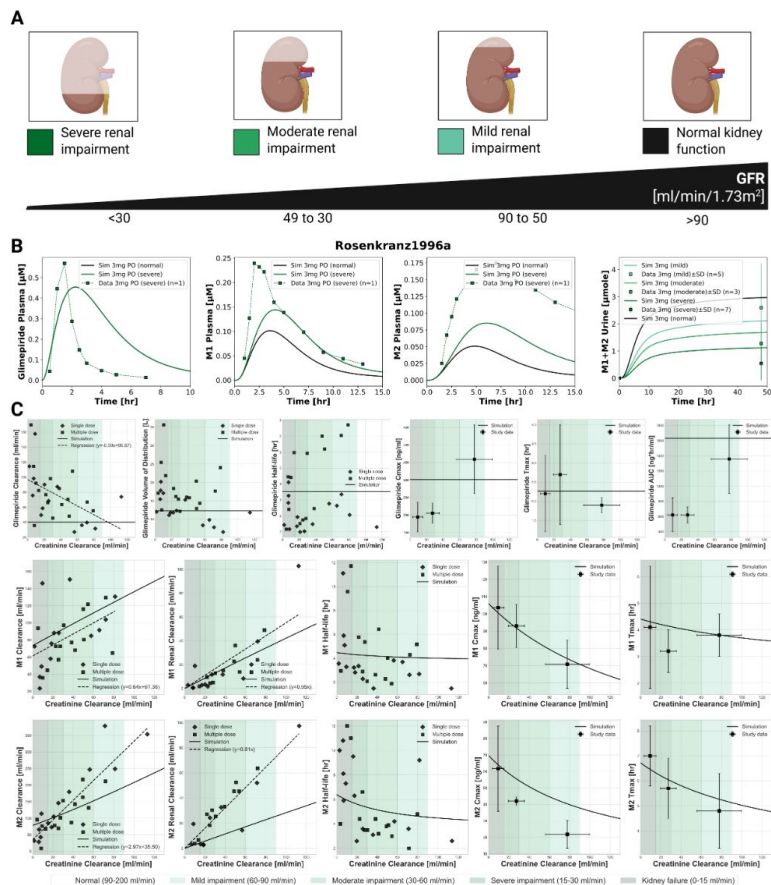


Fig. 3 Impact of renal function on the pharmacokinetics of glimepiride and its metabolites. **A)** Classification of renal function based on Glomerular Filtration Rate (GFR), illustrating normal function, mild, moderate, and severe renal impairment. **B)** Simulated (solid lines) versus observed (symbols) plasma concentration-time profiles for glimepiride, M1, and M2, and cumulative M1+M2 urinary excretion, following a 3 mg oral dose (PO) in subjects with varying degrees of renal function. Observed data from Rosenkranz et al. [28]. **C)** Relationship between creatinine clearance and key pharmacokinetic parameters for glimepiride, M1, and M2, following a 3 mg oral dose (PO). Simulation results (solid lines) are compared with observed clinical data (symbols; dashed lines: regression fits where applicable) from Rosenkranz et al. [28].

Glimepiride - Hepatic Impairment

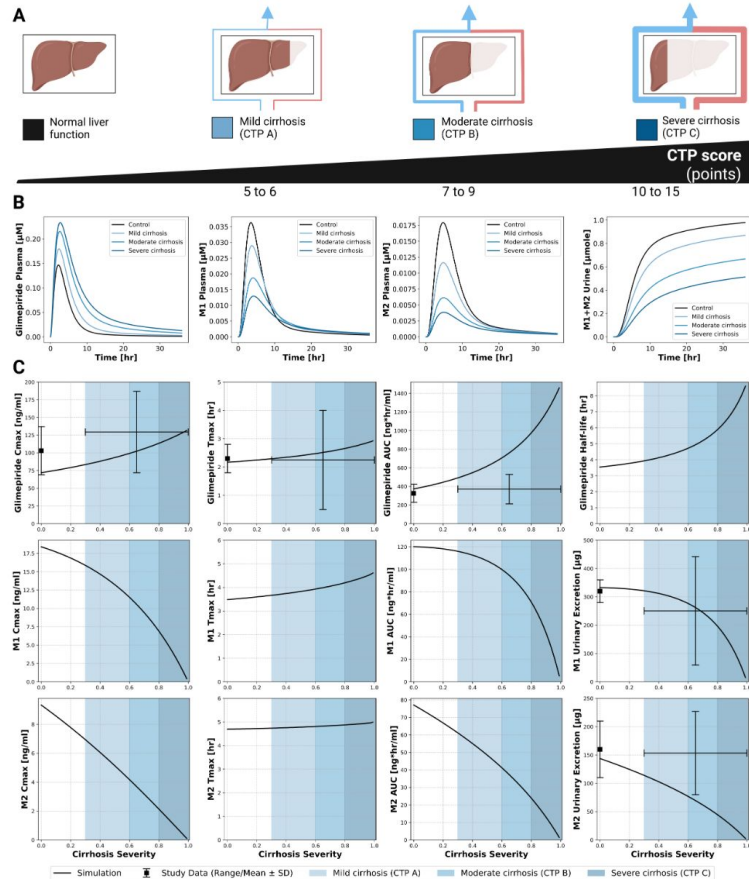


Fig. 4 Impact of hepatic function (cirrhosis severity) on the pharmacokinetics of glimepiride and its metabolites. **A)** Classification of liver function based on the Child-Turcotte-Pugh (CTP) score, illustrating normal function, mild cirrhosis (CTP A), moderate cirrhosis (CTP B), and severe cirrhosis (CTP C). **B)** Simulated plasma concentration-time profiles for glimepiride, M1, and M2, and cumulative M1+M2 urinary excretion, following a 1 mg oral dose in subjects with varying degrees of cirrhosis severity (control, mild, moderate, severe). **C)** Relationship between cirrhosis severity and key pharmacokinetic parameters for glimepiride, M1, and M2, following a 1 mg oral dose. Simulation results (solid lines) are compared with observed clinical data (symbols with error bars where available, representing range/mean±SD) from Rosenkranz et al. [32].

Glimepiride - Bodyweight

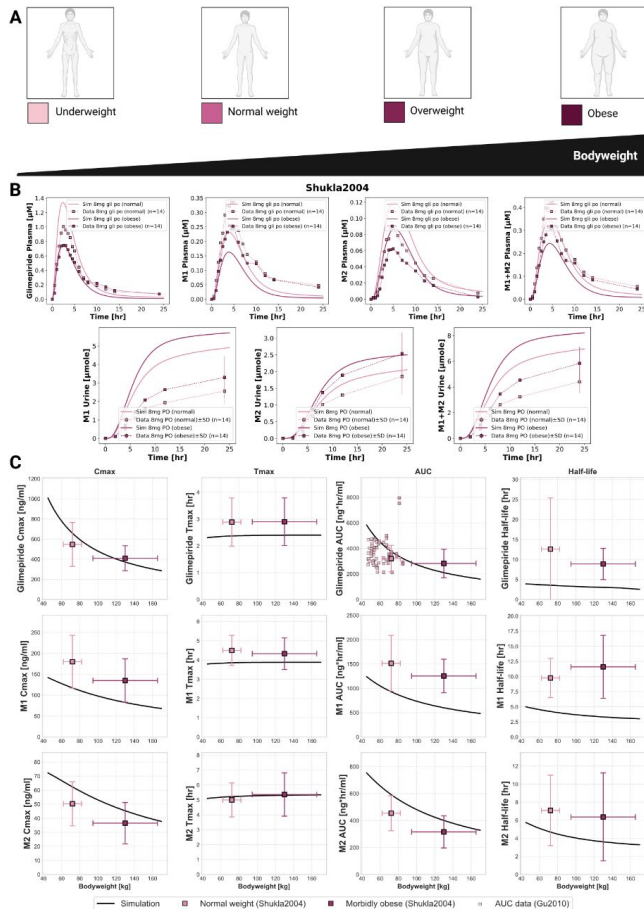


Fig. 5 Impact of bodyweight on the pharmacokinetics of glimepiride and its metabolites. **A)** Illustration of bodyweight categories: underweight, normal weight, overweight, and obese. **B)** Simulated (solid lines) versus observed (symbols) plasma concentration-time profiles and cumulative urinary excretion for glimepiride, M1, and M2, following an 8 mg oral dose (PO) in normal weight and morbidly obese individuals. Observed data from Shukla et al. [29]. **C)** Relationship between bodyweight and key pharmacokinetic parameters for glimepiride, M1, and M2, following a simulated 8 mg oral dose (PO). Simulation results (solid lines) are compared with observed clinical data (squares) from Shukla et al. [29] (8 mg PO, normal weight and morbidly obese groups) and dose-scaled AUC data for glimepiride from Gu et al. [33] (original 2 mg PO dose scaled to 8 mg).

Glimepiride - CYP2C9 Genetic Variants

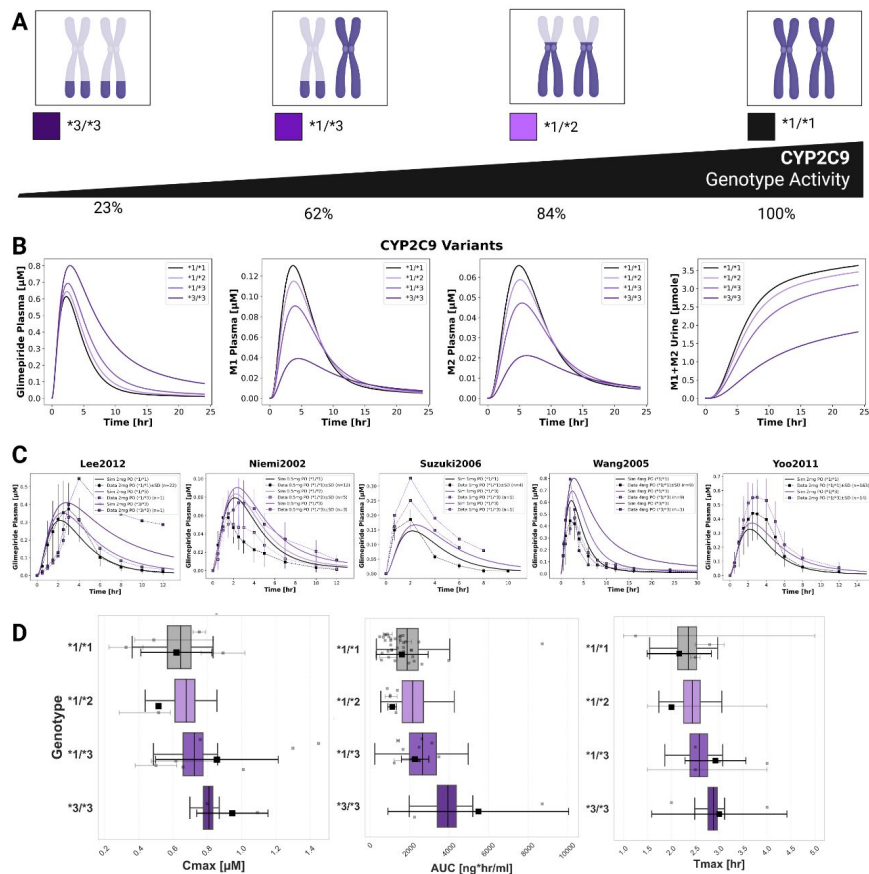


Fig. 6 Impact of CYP2C9 genetic variants on glimepiride pharmacokinetics. **A)** Illustration of key CYP2C9 genotypes (*1/*1, *1/*2, *1/*3, *3/*3) and their corresponding enzymatic activities. **B)** Simulated pharmacokinetic profiles of glimepiride, M1, M2, and cumulative M1+M2 urinary excretion, following a 4 mg oral dose, based on fixed enzyme activity values for different CYP2C9 genotypes. **C)** Comparison of simulated (solid lines, using fixed CYP2C9 activity values) versus observed (symbols) glimepiride plasma concentrations in individuals with different CYP2C9 genotypes across five clinical studies (Lee et al. [22], Niemi et al. [27], Suzuki et al. [30], Wang et al. [31], and Yoo et al. [8]). **D)** Boxplots comparing simulated glimepiride pharmacokinetic parameters derived from the probabilistic sampling approach (colored boxes) with observed clinical data (grey squares: individual data points; black squares: weighted arithmetic mean) across different CYP2C9 genotypes. Simulations for this panel correspond to a 4 mg oral dose. Observed data was aggregated from the clinical studies cited in panel C and dose-scaled to 4 mg where necessary.

Glimepiride - Populations

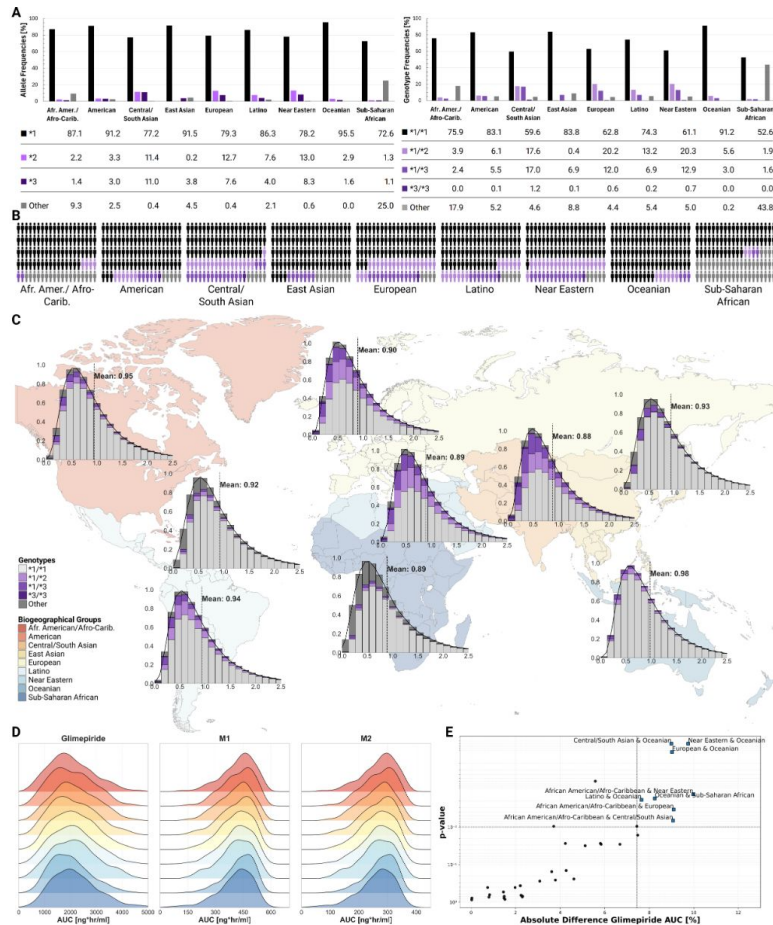
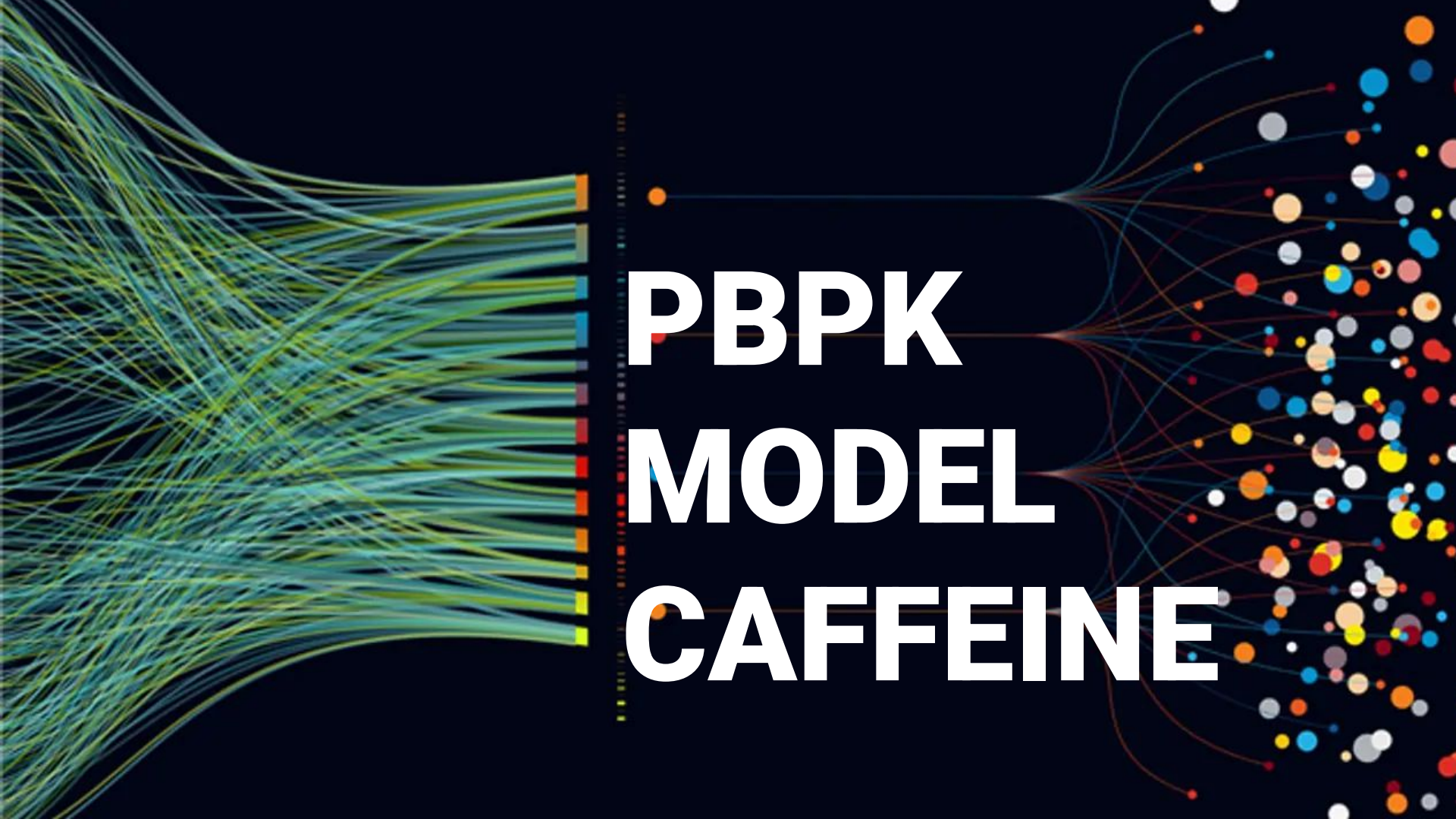
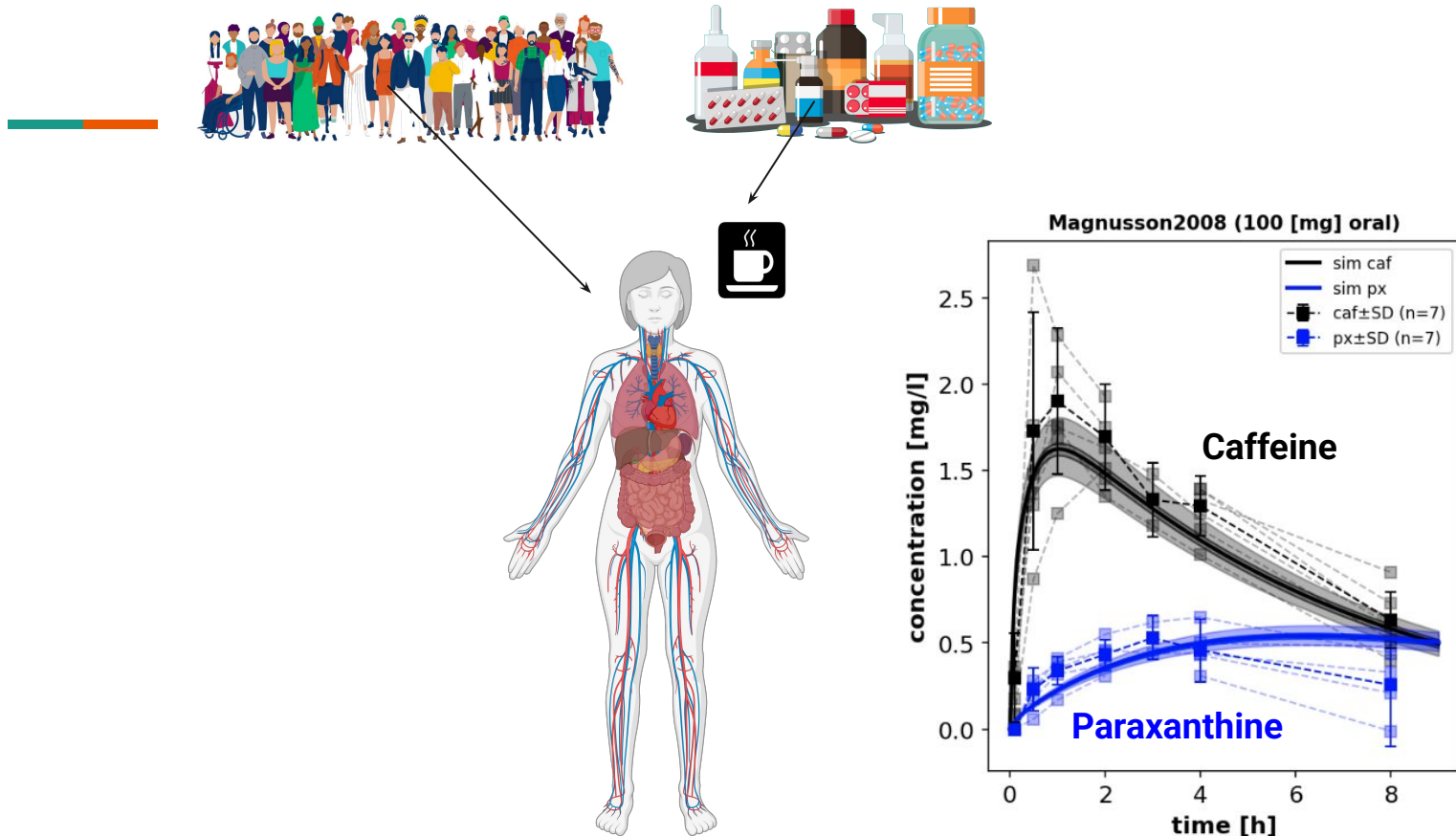


Fig. 7 Global CYP2C9 genetic variability and population-level impact on glimepiride pharmacokinetics. **A)** CYP2C9 allele and genotype frequencies across biogeographical groups [34], showing the distribution of key alleles and genotypes. **B)** Individual genetic variability representation within each biogeographical population. **C)** World map displaying population-specific CYP2C9 activity distributions derived from allele frequencies, with kernel density estimation (KDE) curves and mean enzymatic activity values shown for each biogeographical group. **D)** Ridgeline plots comparing glimepiride, M1, and M2 AUC distributions across biogeographical populations. **E)** Statistical comparison of population pairs showing the relationship between significance (p-value) and magnitude of pharmacokinetic differences, with some comparisons showing statistically significant but clinically modest differences in glimepiride AUC.

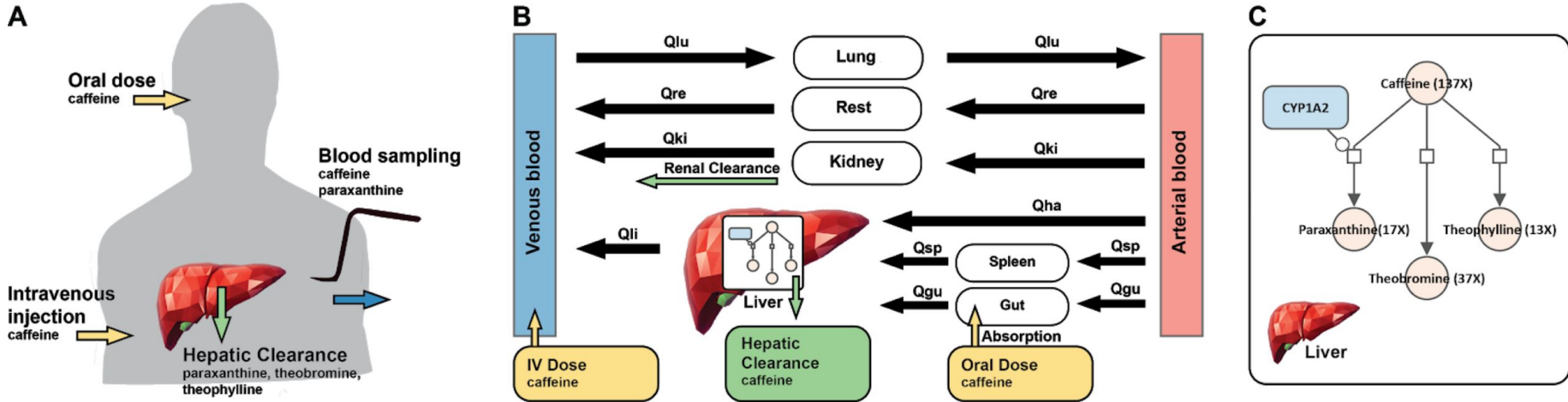
The background is a dark blue gradient. On the left, a dense cluster of thin, flowing lines in shades of green, teal, and blue curves towards the center. On the right, a network of thin lines connects numerous small, colorful circles in various sizes and colors (blue, orange, yellow, red, grey, white).

PBPK MODEL CAFFEINE

Pharmacokinetics of drugs



PBPK Model of Caffeine

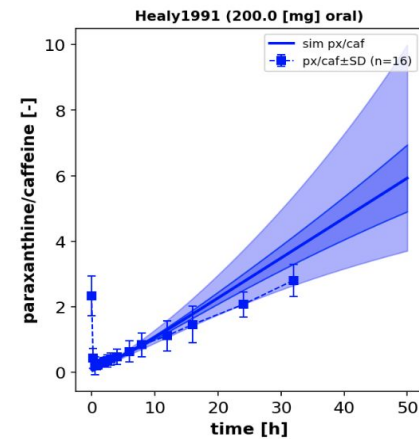
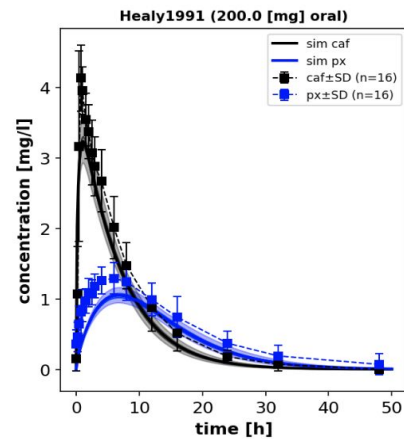
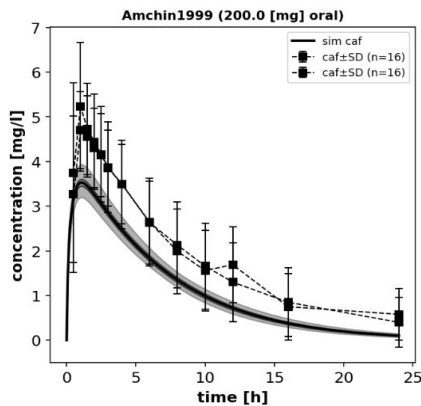
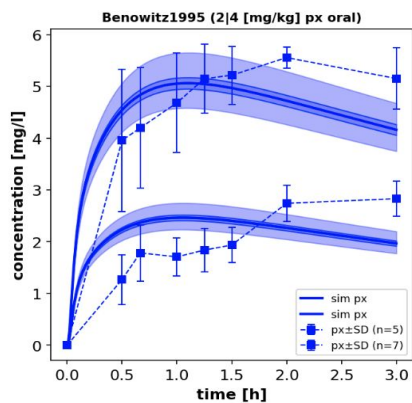
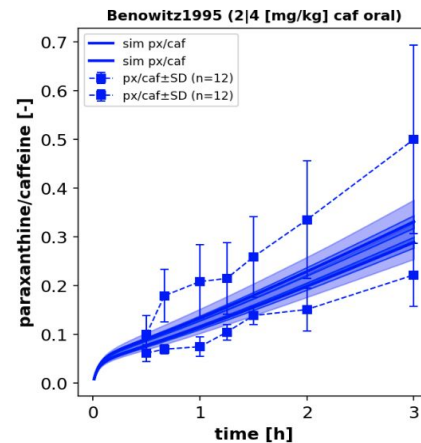
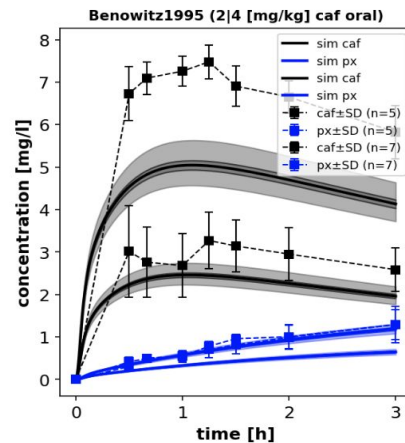
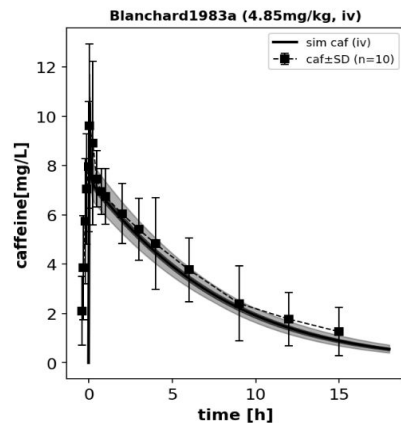
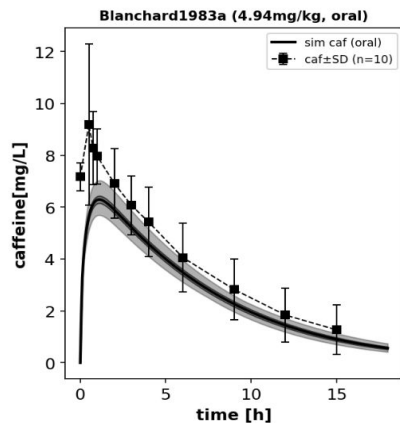


- Caffeine metabolized by **CYP1A2** to paraxanthine,
- Classical liver function test
 - Time course of caffeine
 - Caffeine/paraxanthine ratio

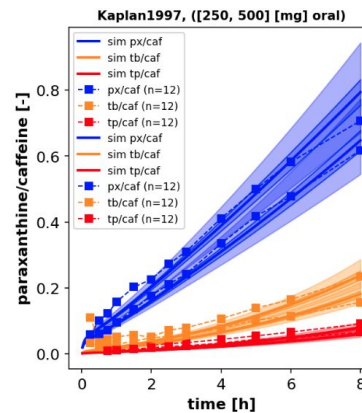
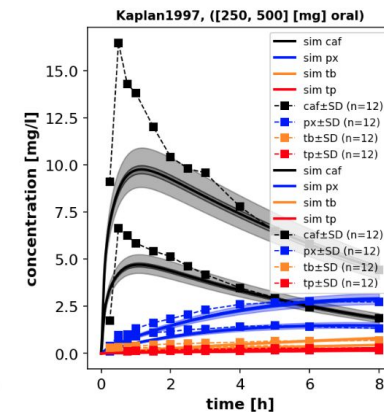
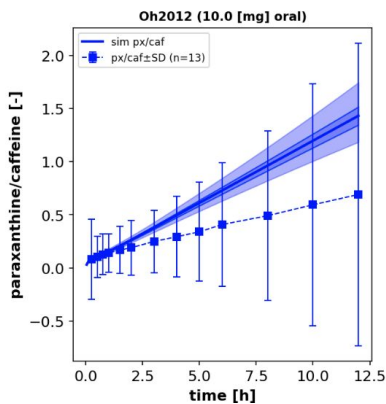
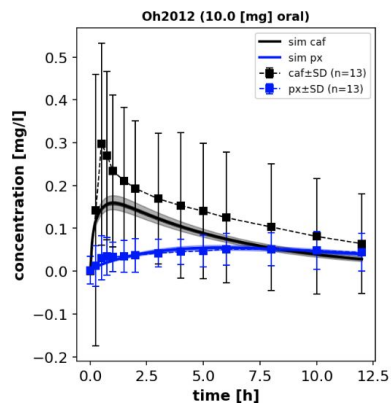
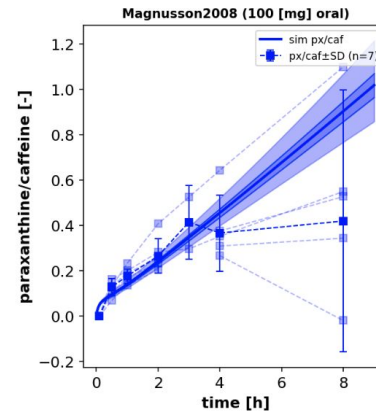
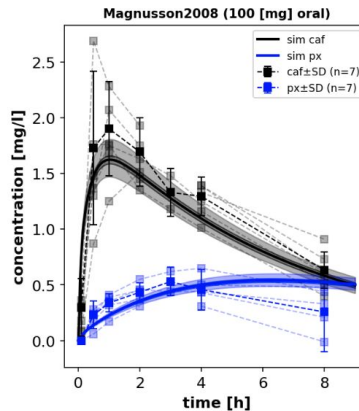
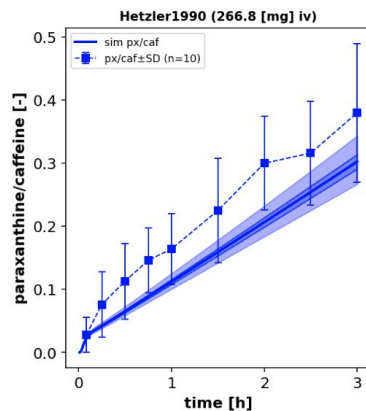
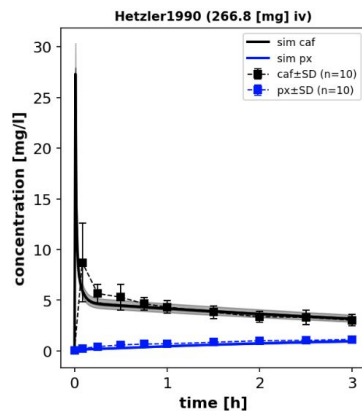
Challenges

- Large inter-subject variability
 - Effects of lifestyle on expression (induction smoking)
 - Effects of medication (oral contraceptives)
- Dose dependency

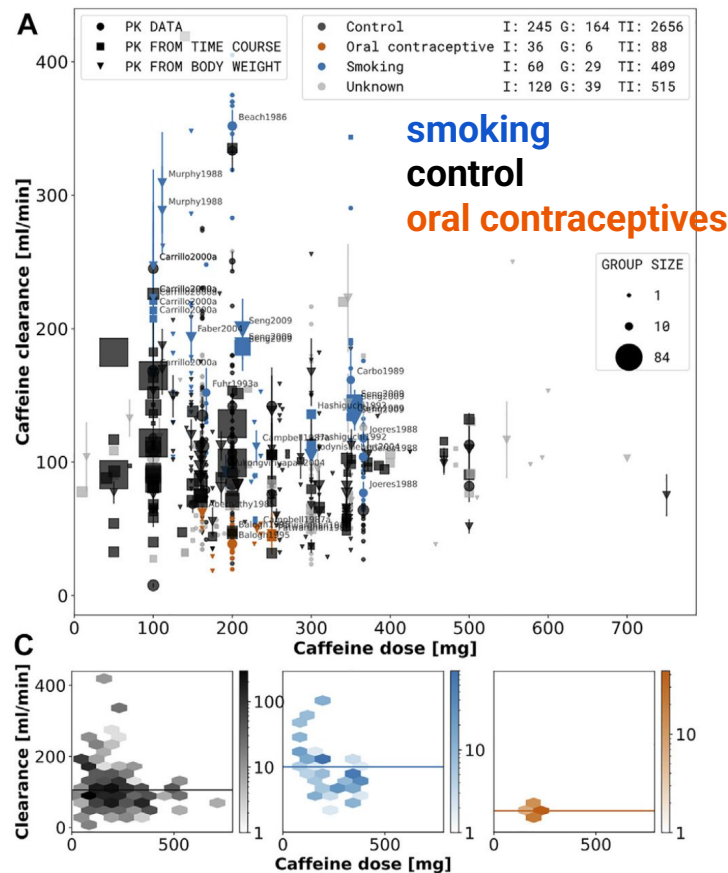
Model Performance (Training)



Model Performance II (Training)



Lifestyle: Smoking & Oral Contraceptives



- Smoking induces caffeine clearance
- Oral contraceptives reduce

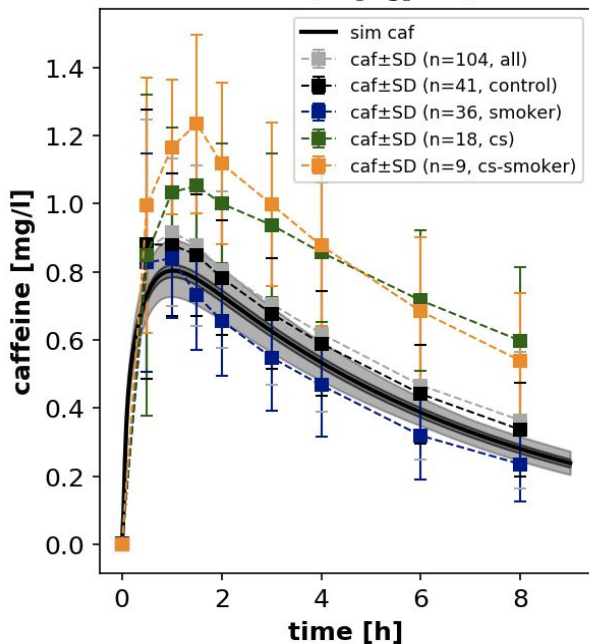
J.Grzegorzewski, F.Bartsch, A.Köller, and M.König
Pharmacokinetics of caffeine: A systematic analysis of reported data for application in metabolic phenotyping and liver function testing
 Frontiers in Pharmacology 2022, Vol12; doi: [10.3389/fphar.2021.752826](https://doi.org/10.3389/fphar.2021.752826)

Grzegorzewski J, Brandhorst J, Green K, Eleftheriadou D, Duport Y, Barthorscht F, Köller A, Ke DYJ, De Angelis S, König M.

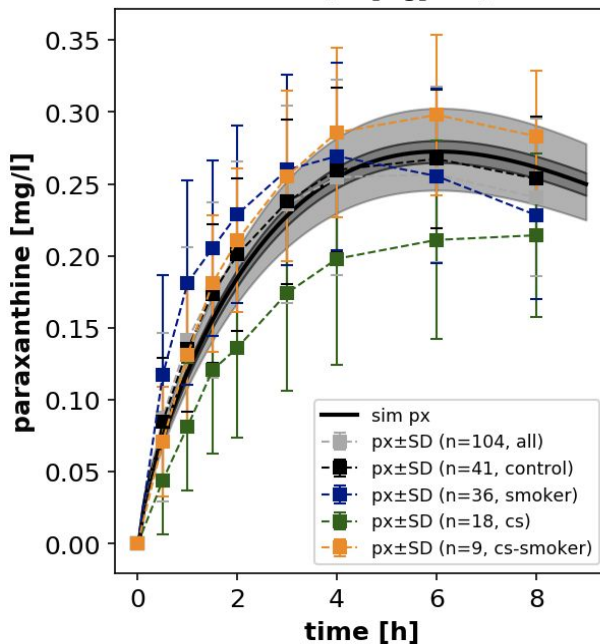
PK-DB: pharmacokinetics database for individualized and stratified computational modeling
 Nucleic Acids Res. 2020 Nov 5;gkaa990. doi: [10.1093/nar/gkaa990](https://doi.org/10.1093/nar/gkaa990).

Stratification by Smoking & Contraceptives

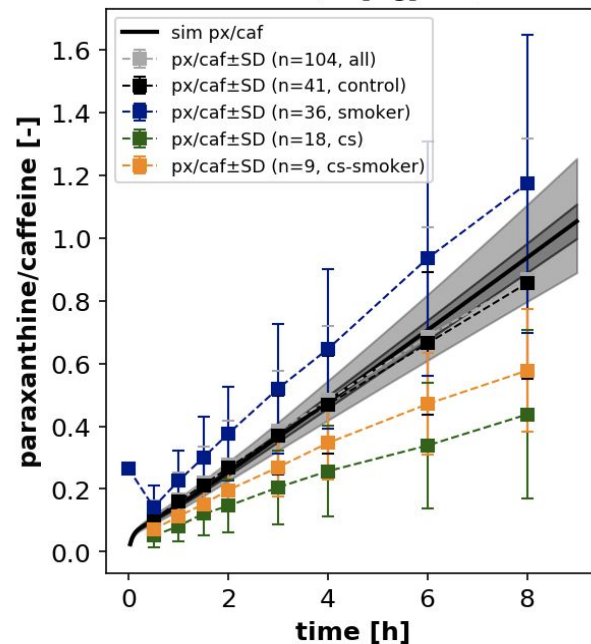
IKP243 (50 [mg] oral)



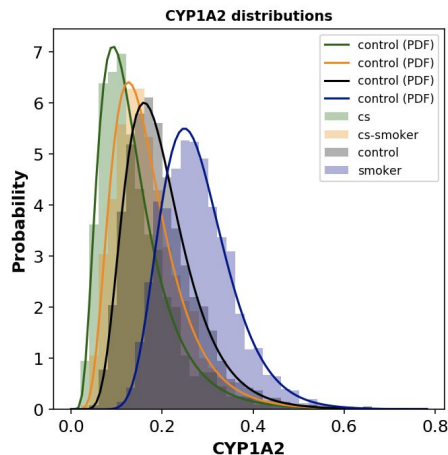
IKP243 (50 [mg] oral)



IKP243 (50 [mg] oral)

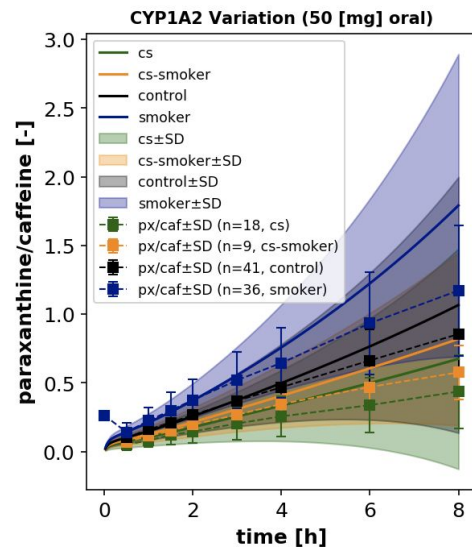
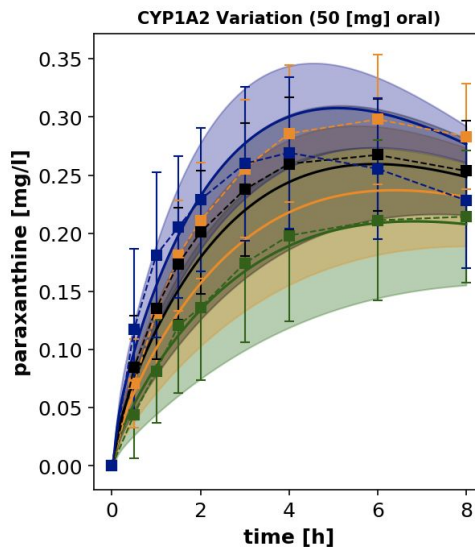
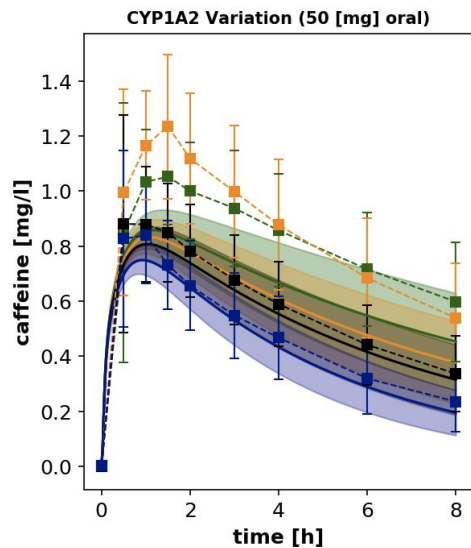


- contraceptives (cs)
- contraceptives-smoker (cs-smoker)
- control
- smoker

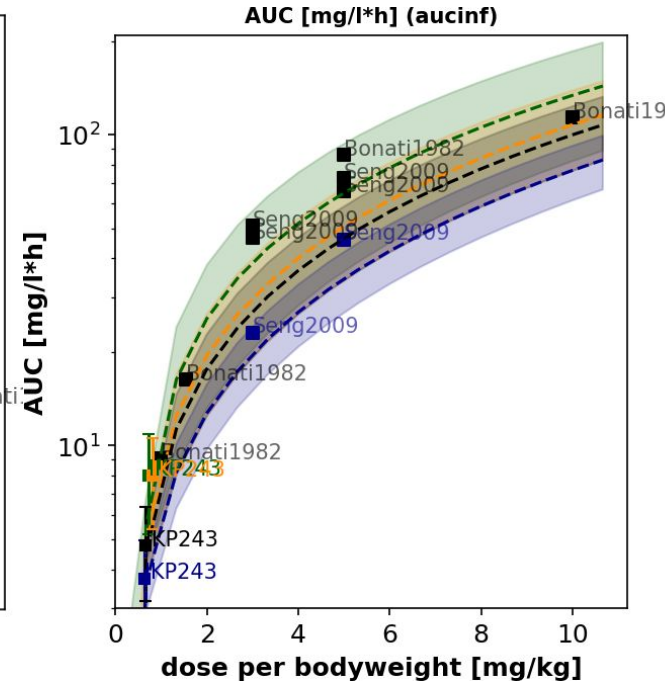
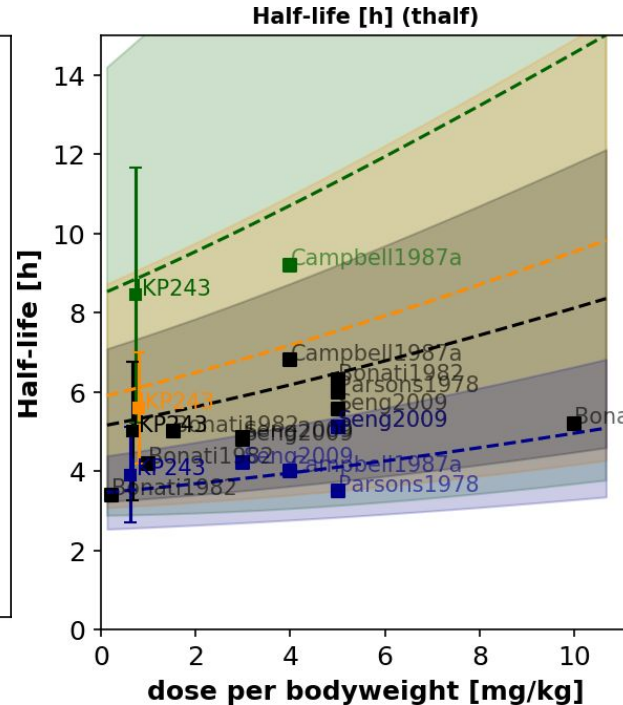
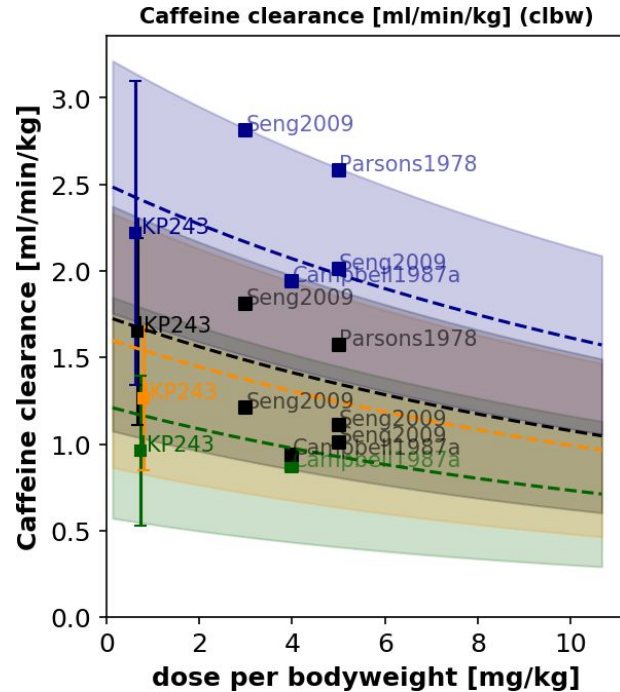


CYP1A2 Distributions

- contraceptives (cs)
- contraceptives-smoker (cs-smoker)
- control
- smoker

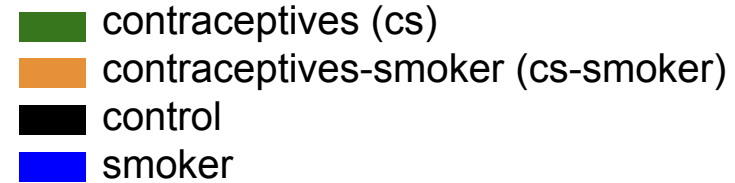
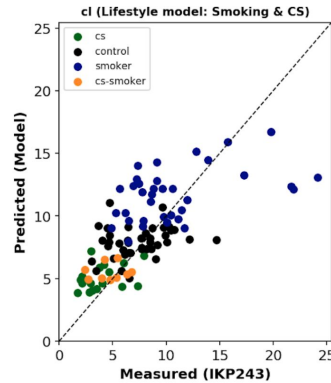
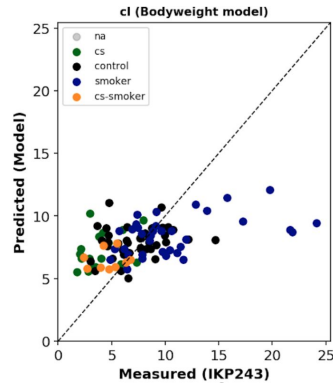
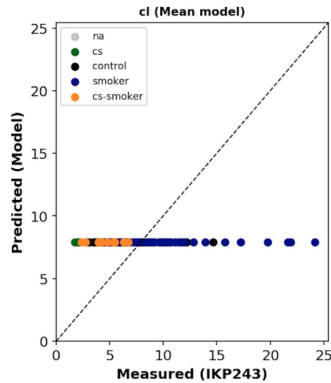


Stratified Dose-Dependent Pharmacokinetics (Validation)



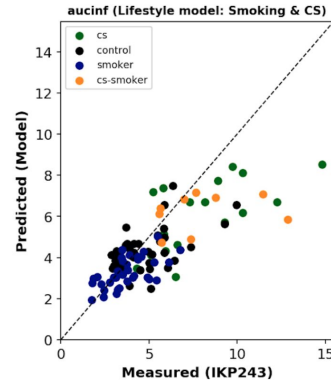
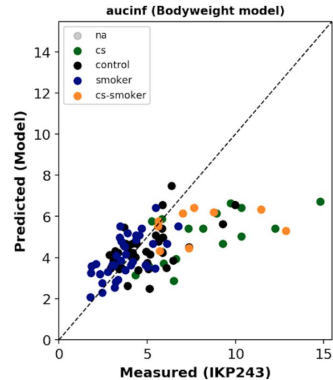
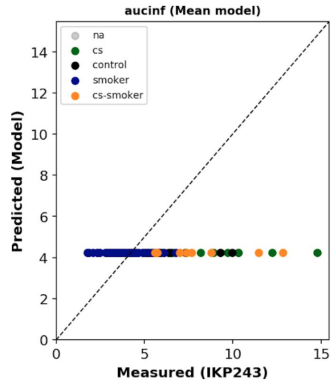
Individualized Predictions

Clearance



- Improved predictions of pharmacokinetic parameters by account for individual lifestyle factors (smoking)

AUC



- Results directly transfer to all drugs metabolized via CYP1A2

mean

anthropometric

lifestyle

CYP1A2 & Caffeine Pharmacokinetics

- CYP1A2 expression altered by many lifestyle factors
- Strong effect: **Smoking**
- Altered function test results

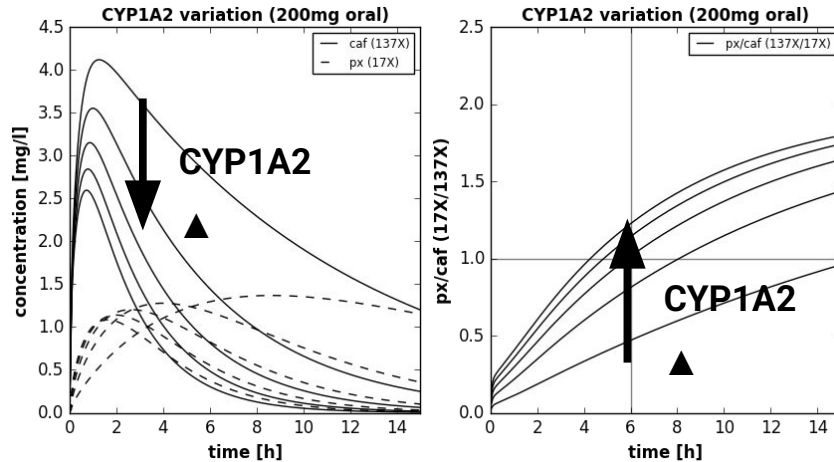


Table 4. Parameter estimates of covariates obtained for logarithmic clearance values using the paraxanthine/caffeine ratio method (equation 1)

Covariate	Symbol used in equation 5	Estimate	95% Confidence interval		Mean resulting change of clearance (factor)
			Lower bound	Upper bound	
–	Intercept	0.264	–0.015	0.542	–
Coffee intake (litre day ⁻¹)	Slope _{coffee}	0.368	0.287	0.449	1.445
Body mass index (kg m ⁻²)	Slope _{BMI}	–0.010	–0.018	–0.002	0.990
Cigarettes/day					
Non-smokers	V _{smoking habit index}	0	–	–	Reference
1–5		0.195	0.065	0.324	1.215
6–10		0.383	0.253	0.509	1.467
11–20		0.504	0.386	0.621	1.655
>20		0.543	0.430	0.655	1.721
Oral contraceptives					
No	V _{oral contraceptive index}	0	–	–	Reference
Yes		–0.332	–0.236	–0.428	0.717
Country					
Germany	V _{country of residence index}	0	–	–	Reference
Bulgaria		–0.209	–0.356	–0.061	0.811
Slovakia		–0.303	–0.450	–0.156	0.739
Sex					
Male	V _{sex index}	0	–	–	Reference
Female		–0.111	–0.178	–0.044	0.895

CYP1A2 induction ▲

- Clearance ▲
- k_{el} ▲
- $T_{1/2}$ ▼
- T_{max} ▼
- $px(17X)/caf(137X)$ ▲